

---

# Bulk composition of a zoned rare-earth minerals-bearing pegmatite in the Pikes Peak granite batholith near Wellington Lake, central Colorado, U.S.A.

Markus B. Raschke<sup>1\*</sup>, Charles R. Stern<sup>2\*</sup>, Evan J. D. Anderson<sup>1</sup>, M. Alexandra Skewes<sup>2</sup>, G. Lang Farmer<sup>2</sup>, Julien M. Allaz<sup>3</sup>, and Philip M. Persson<sup>4</sup>

<sup>1</sup>*Department of Physics, Department of Chemistry, and JILA, University of Colorado, Boulder, CO 80309, U.S.A.*

<sup>2</sup>*Department of Geological Sciences, University of Colorado, 399-UCB, Boulder, CO 80309, U.S.A.*

<sup>3</sup>*ETH Zürich, Department of Earth Sciences, Institute of Geochemistry and Petrology, Clausiusstrasse 25, 8092 Zürich, Switzerland*

<sup>4</sup>*Department of Geology and Geological Engineering, 1516 Illinois St., Colorado School of Mines, Golden, CO 80401, U.S.A.*

\*Correspondence should be addressed to: markus.raschke@colorado.edu and charles.stern@colorado.edu

---

## ABSTRACT

A previously undescribed small lenticular ( $\sim 5 \times 5 \times 5$  m) pegmatite, located near Wellington Lake in the NW part of the 1.08 Ga 'A-type' (anorogenic) ferroan Pikes Peak granite batholith,  $\sim 15$  km SW of the South Platte pegmatite district in central Colorado, is concentrically zoned around a mostly monomineralic quartz core with interconnected miarolitic cavities. Major constituents of the Wellington Lake pegmatite are quartz, perthitic microcline, albite (variety cleavelandite), hematite, and biotite. Accessory minerals include fluocerite, bastnäsite, columbite, zircon (var. 'cyrtolite'), thorite, and secondary U phases. Fluorite is conspicuously absent, although it is a common phase in the South Platte district NYF-type pegmatites, which are rich in niobium (Nb), yttrium (Y), fluorine (F), and heavy rare-earth elements (HREE). Notable for the Wellington Lake pegmatite are a small quantity of well-developed tabular crystals of fluocerite that reach up to 4 cm in diameter, with sub-mm epitaxial bastnäsite overgrowths, suggesting formation from F- and CO<sub>2</sub>-bearing solutions rich in light rare-earth elements (LREE), with decreasing  $a(\text{F}^-)/a(\text{CO}_3^{2-})$  during the last crystallization phase. An Nd-isotope value of  $\epsilon_{\text{Nd1.08Ga}} = -1.6$  for the fluocerite is within the range of  $\epsilon_{\text{Nd1.08Ga}} = -0.2$  to  $-2.7$  of the host coarse-grained, pink K-series Pikes Peak Granite (PPG), indicating that REE and other pegmatite constituents derived from the parental PPG magma. A calculation of total pegmatite composition based on whole-rock chemistry and volume estimates of the different pegmatite zones reveals an overall composition similar to the PPG with respect to Si, Al, Na, and K. Yet the pegmatite is depleted in Fe, Mg, Ca, Ti, Mn, and P, the high-field-strength elements (HFSE; Zr, Hf, Nb, Y, Th), and, most significantly, total REE compared to the PPG. Despite containing the LREE minerals fluocerite and bastnäsite, the lack of a net overall REE enrichment of the pegmatite compared to the PPG reflects the large amount of REE-poor silicate minerals forming the wall, intermediate, and core zones of the pegmatite. The calculated total pegmatite composition suggests that the pegmatite formed by the separation from the PPG magma of an F-poor H<sub>2</sub>O-saturated silicate melt depleted in REE

and HFSE compared to the F-rich melts, which formed the NYF-type HREE-rich ( $\text{La}_N/\text{Yb}_N < 1$ ) pegmatites in the South Platte district. Homogenization temperatures of  $< 500^\circ\text{C}$  for possibly primary fluid inclusions in large quartz crystals from the core of the Wellington Lake pegmatite are consistent with recent models of pegmatite petrogenesis leading to nucleation controlled mega-crystal growth resulting from supercooling.

**KEY WORDS:** Colorado, fluocerite, Pikes Peak granite batholith, rare-earth elements, South Platte pegmatite district, Wellington Lake pegmatite.

## INTRODUCTION

The petrogenesis of granitic pegmatites has been a subject of debate to consistently explain their characteristic features, notably textural and mineralogical heterogeneity, inward coarsening and oriented crystal growth, distinct zonation of mineral assemblages, and their mineralogical and geochemical diversity (Swanson, 1977; Simmons and Webber, 2008; London,

2008, 2009, 2014, 2015, 2016, 2018; Thomas et al., 2012; Thomas and Davidson, 2015; Sirbescu et al., 2017). Although pegmatites are generally established to be of igneous origin, the role of late-stage hydrothermal processes is often hard to either discount or discern.

Few studies have systematically addressed the bulk composition of pegmatites, because of the difficulties associated with exposure, internal zoning, and paragenetic heterogeneity (Gordienko, 1996; Zagorsky et al., 1997). Two recent notable exceptions are for the very large, complexly zoned, rare-earth element (REE) and Li-, Cs-, and Ta-rich (LCT-type) Tanco pegmatite at Bernic Lake in southeast Manitoba (Stilling et al., 2006), and the smaller Mount Mica LCT-type pegmatite dike in southwest Maine (Simmons et al., 2016). Whereas the Mount Mica study suggests a derivation by the anatexis of the host rocks for this pegmatite, the Tanco pegmatite work supports an origin from a parental granitic magma.

Another class of pegmatites of particular interest in Colorado are those associated with 'A-type' (anorogenic; Eby, 1990; Černý and Ercit, 2005; London, 2008) ferroan (Frost and Frost, 2011) granites, such as those in the South Platte pegmatite district at the northern end of the 1.08 Ga Pikes Peak granite batholith (Smith et al., 1999; our Fig. 1). This district has long been known for its abundant pegmatites, which locally are quite large (as large as ca. 50 m in width), and commonly contain unusual REE minerals and zoned mineral assemblages (Simmons and Heinrich, 1975, 1980; Simmons et al., 1987; Allaz et al., 2020). Several of the pegmatites in the central part of the South Platte district contain locally abundant HREE-rich minerals. They are well described examples of NYF-type (gadolinite subtype) pegmatites, which are characteristically rich in Nb, Y, F, and HREE, and commonly associated with 'A-type' ferroan granites (Eby, 1990; Černý and Ercit, 2005).

Early studies suggest that the South Platte pegmatites formed from the crystallization of a late-stage, volatile-rich magma of the Pikes Peak granite batholith (Haynes, 1965). However, aspects of the origin and formation of the South Platte pegmatites still remain unclear, specifically whether the REE-rich minerals in these pegmatites are the result of an already REE-enriched parental granitic magma (Simmons and Heinrich, 1980), result of extreme fractionation concentrating REE during pegmatite crystallization, or result from an influx of REE-rich fluids unrelated to the Pikes Peak Granite (PPG) (Gagnon et al., 2004). For the Oregon #3 pegmatite in the South Platte pegmatite district (Fig. 1), Simmons and Heinrich (1980) noted that although the PPG is enriched in total REE relative to many other granites, the total REE content of the pegmatite seems ~10× above the PPG value. However, although the PPG is enriched in LREE relative to HREE ( $La_N/Yb_N = 10$ ), the Oregon #3 pegmatite appears to be enriched in HREE relative

to LREE, with  $La_N/Yb_N < 1$ . This implies that processes involving fractionation of HREE relative to LREE, rather than simple overall enrichment in total REE relative to the granite, must be considered in the formation of the Oregon #3 and other South Platte NYF-type pegmatites.

In contrast to the large NYF-type pegmatites in the central part of the South Platte district, pegmatites in the southern and western part of the batholith are mostly smaller in size (< 1 m to 15 m diameter) and often contain the LREE-rich minerals allanite and monazite. In this work we investigate an example of one of these smaller, internally zoned, LREE mineral-bearing pegmatites, located northwest of Wellington Lake (Fig. 1). This Wellington Lake pegmatite has not been previously described. To understand the chemical, textural, and mineralogical attributes of this pegmatite, we undertook mapping and transect sampling of the pegmatite, thin-section petrography, and whole-rock chemical analysis of the individual pegmatite zones via bulk sampling. Additionally, petrographic and thermometric analyses of fluid inclusions in quartz from the pegmatite core zone were performed, along with quantitative mineral analysis of the LREE-rich minerals in the pegmatite core. Finally, Nd-isotope data were obtained to determine if the pegmatite magma source was the magma that formed the PPG hosting the pegmatite.

## GEOLOGIC SETTING

Figure 1 shows the geologic setting with the Wellington Lake pegmatite (lat. 39.322855°S, long. 105.399503°W) situated as an outlying body southwest of the central South Platte pegmatite district. The Wellington Lake pegmatite is located ~3 km northwest of Wellington Lake and ~2 km southeast of the McGuire pegmatite (Fig. 1), which is a large, irregularly zoned NYF-type pegmatite (Černý et al., 1999). Field work around the Wellington Lake pegmatite revealed several other pegmatites as isolated bodies or swarms. Most notably, ~500 m to the SW of the Wellington Lake pegmatite, a group of smaller, well-exposed granite-hosted pegmatites crop out. These contain fluorite in miarolitic cavities in their quartz cores, but lack apparent REE mineralization.

The Wellington Lake pegmatite is a steeply dipping, lenticular body hosted in medium- to coarse-grained, pink syenogranite corresponding to the major K-series phase of the Pikes Peak granite batholith. It is partially exposed in vertical cross section in an ~10-m-tall, steep west-facing outcrop, in sharp contact with minimally weathered pink syenogranite on at least three sides in its exposure (Fig. 2). The pegmatite body consists of a main, roughly prolate, ellipsoidal body ~4 m in diameter. It is exposed in a frontal plane with an upper zone over a vertical extent of ~3 m. Figure 2A shows a cross section of the upper miarolitic zone.

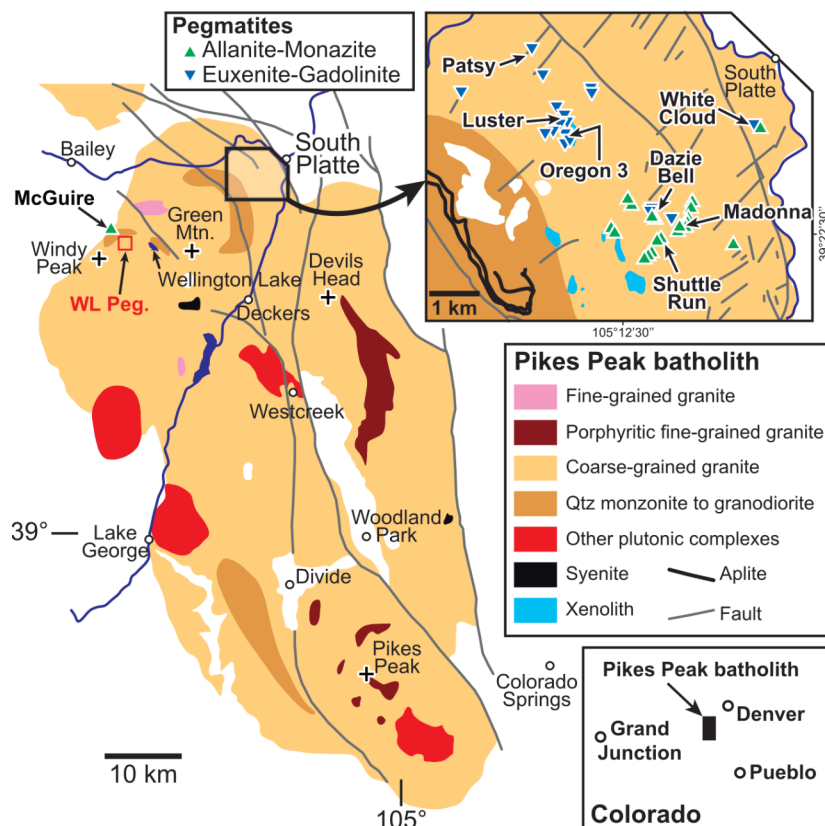


Figure 1. Geologic map of the Pikes Peak granite batholith (Colorado) with the location of the Wellington Lake pegmatite (red square, WL peg.) relative to Wellington Lake, the McGuire pegmatite, and the South Platte pegmatite district (inset), within which occur the Oregon #3, the White Cloud, and other major NYF-type pegmatites (after Barker et al., 1975, 1976; Smith et al., 1999).

The pegmatite has recently been prospected for its large milky and smoky quartz crystals, which are abundant in the core zone of the pegmatite.

### Wall Zone

As seen in cross sections B and C of Figure 2A, the host granite is in sharp contact with a narrow (~10-cm-wide) wall zone of graphic granite. The wall zone represents about 20 vol. % of the pegmatite (Fig. 2).

### Intermediate Zone

The wall zone then transitions into an ~95-cm-wide intermediate zone, which represents about 69 vol. % of the pegmatite. First is a coarser-grained ~20-cm-wide outer intermediate zone (OIZ) of graphically intergrown quartz and microcline-perthite with minor biotite laths. We estimate that the OIZ represents about 22 vol.

% of the pegmatite (Fig. 2). Proceeding inward, the OIZ is in contact with an ~60-cm-wide middle intermediate zone (MIZ) composed of a still coarser graphic quartz and microcline-perthite without biotite. The MIZ represents ~41 vol % of the pegmatite. This zone is followed inward by an ~15-cm-wide inner intermediate zone (IIZ), which is characterized by microcline-perthite and small laths of albite, without quartz, along with irregular pods of ‘cleavelandite’ albite, biotite, and hematite. We estimate that the IIZ represents ~6 vol. % of the pegmatite.

### Core Zone

The core zone consists of an ~2-m-diameter quartz core with open cavities lined with anhedral to euhedral, multi-generation milky and smoky quartz crystals as large as ca. 50 cm in size. Open spaces are partially filled with minor hematite, albite, and clay

minerals. The core represents about 11% of the pegmatite volume. Mirolitic cavities within the core form void space in druses and between large quartz crystals. These constitute < 0.5 vol. % of the total pegmatite.

Accessory minerals in the pegmatite include fluorite and bastnäsite in the core, and columbite, ‘cyrtoilite’ zircon, thorite, and minor secondary U–Th species in the IIZ. Notable is the absence of fluorite or phosphate minerals (e.g., monazite, xenotime, or apatite) in any of the zones of the pegmatite body.

### METHODS

Thin sections were examined, and bulk chemistry determined (Figs. 3 and 4) for samples across the transition from the granite into the core of the pegmatite (Fig. 2; Tables 1–3). Inductively coupled plasma-mass spectrometry (ICP-MS) trace-element and whole-rock major element compositions were obtained from Activation Laboratories Ltd. (Ontario, Canada).

Mineral chemistry was determined by electron microprobe (EMP) analysis using a JEOL JXA-8600 EMP at the University of Colorado Boulder. It is a four-spectrometer instrument equipped with argon X-ray detectors (P-10 mixture) on spectrometers 1 and 2 (PET and TAP crystals), and xenon X-ray detectors on spectrometers 3 and 4 (LiF crystals). Operating conditions using a W-cathode were 15 KV accelerating potential with a 20 nA probe current. Details on EMP analy-

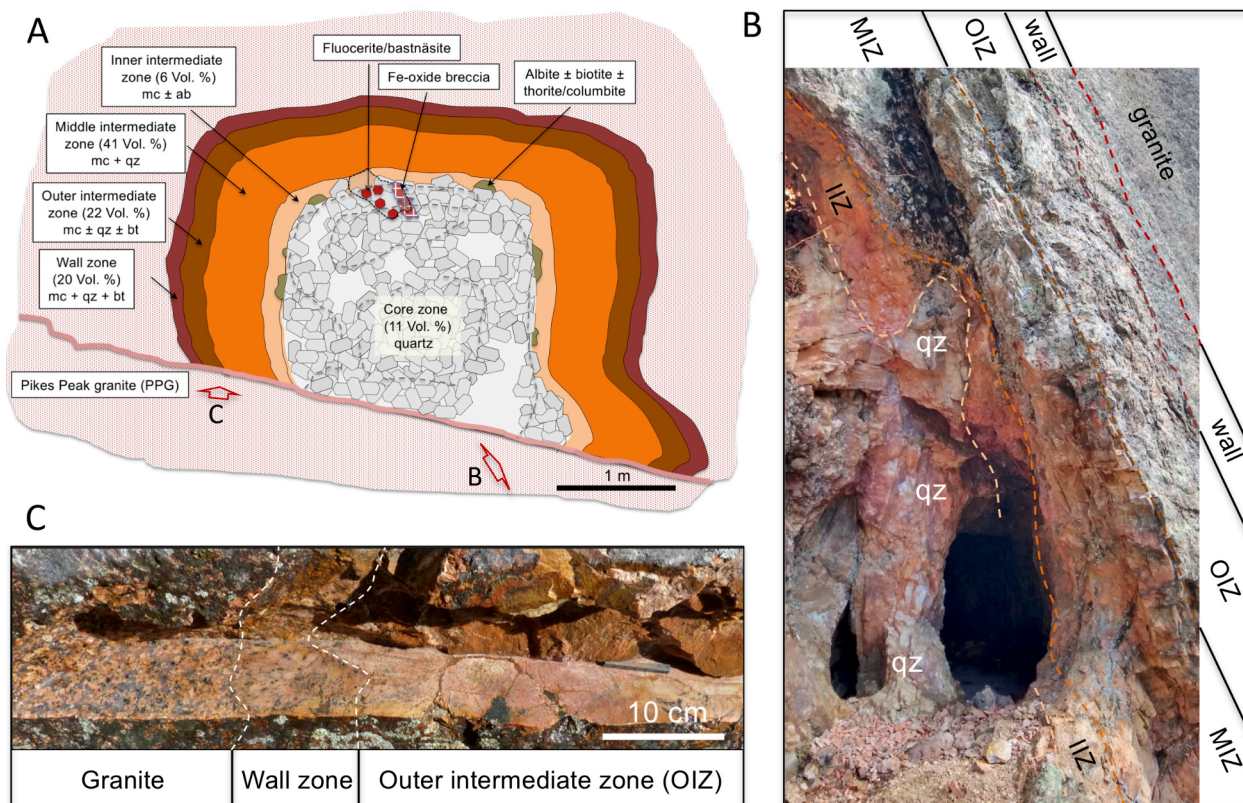


**Figure 2.** *A*, Cross section of the Wellington Lake pegmatite zones. Abbreviations: ab = albite, bt = biotite, mc = microcline-perthite, qz = quartz. *B*, View of the right (south) side with the different pegmatite zones (OIZ = outer intermediate zone; MIZ = middle intermediate zone; IIZ = inner intermediate zone), and quartz core with interconnected miarolitic openings providing sampling access. *C*, Saw cut of left (north) side of the granite-pegmatite contact with sharp transition from Pikes Peak granite to the fine-grained thin graphic wall zone into the coarse-grained OIZ.

sis and standards used for the REE minerals fluocerite and bastnäsite are described in Allaz et al. (2015, 2020).

Micro-Raman spectroscopy on polished thin sections was performed on an upright Raman microscope (Olympus BH51, with 632 nm HeNe laser excitation at 1 mW, a 50× objective of NA = 0.8, and a Princeton Instruments Acton SP500a imaging spectrograph, with a PIXIS 100 liquid nitrogen-cooled CCD camera, calibrated on multiple spectral lines using a He-lamp). Nd-isotopic data were obtained using established analytical procedures (Farmer et al., 1991). Measured  $^{143}\text{Nd}/^{144}\text{Nd}$  was normalized to  $^{146}\text{Nd}/^{144}\text{Nd} = 0.7219$ . The Nd-isotopic compositions are reported as  $\epsilon_{\text{Nd}}$  values using a reference  $^{143}\text{Nd}/^{144}\text{Nd}$  ratio of 0.512638.

Fluid-inclusion petrography and thermometry were performed on doubly polished thin sections of quartz from the top of the core of the pegmatite. Inclusions were analyzed thermometrically with an adapted U.S. Geological Survey gas-flow heating stage. Stage calibration was carried out at  $-56.6^\circ\text{C}$ ,  $0.0^\circ\text{C}$ , and  $374^\circ\text{C}$ , using synthetic fluid inclusion (SYN FLINC) standards. Uncertainties in the ther-

momeric measurements are  $\pm 0.2^\circ\text{C}$  at  $0.0^\circ\text{C}$ , and  $\pm 3^\circ\text{C}$  at  $374^\circ\text{C}$ . Salinities were determined from thermometric measurements as described by Potter et al. (1977, 1978).

## PETROLOGY AND CHEMISTRY

### Granite

The coarse-grained, pink K-series Pikes Peak Granite (PPG) that hosts the pegmatite consists of quartz, perthitic microcline and orthoclase, and Fe-rich mica (annite), with minor plagioclase and accessory magnetite, zircon, fluorite, and trace monazite. Its mineralogy is typical for coarse-grained pink Pikes Peak granite, but lacks amphibole, which has been observed in small quantities in other K-series Pikes Peak granite samples elsewhere in the batholith (Simmons and Heinrich, 1980; Simmons et al., 1987; Smith et al., 1999). Three samples of granite, WL-19, WL8-1, and WL8-2 (Table 1), are similar in composition to previously published analyses (Smith et al., 1999). They have 600 to 800 ppm total REE, which is relatively high

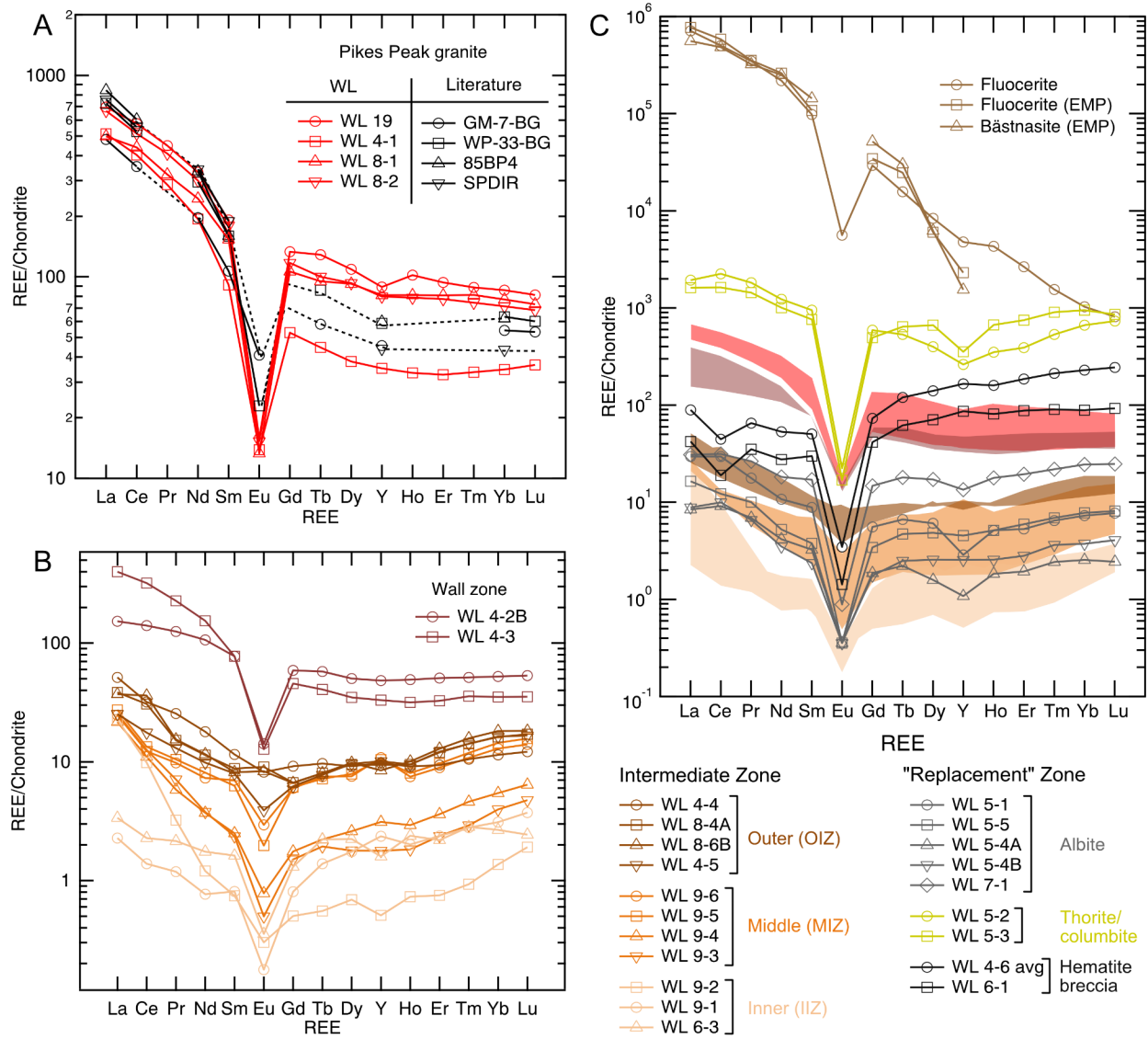


**Figure 3.** Whole-rock REE contents of: *A*, host coarse pink Pikes Peak granite; *B*, pegmatite zones from the wall zone, through the outer, middle, and inner intermediate zones (OIZ, MIZ, and IIM); and *C*, samples from the “replacement zone” of albite, thorite, and columbite bearing rock, and the hematite breccia. Fluocerite ICP-MS analyses, as well as fluocerite and bastnäsite electron microprobe (EMP) analyses are also plotted in *C*. Fields in *C* have the same colors as the individual samples in *A* (red for the granite), and *B* (shades of brown for the wall and intermediate zones). Note the continuous inward REE depletion, yet increasing  $La_N/Yb_N$ , and the HREE enrichment in the hematite breccia and albite, thorite, and columbite bearing rocks of the “replacement zone,” in contrast to and compensated by the LREE-rich mineral phases.

compared to other granites worldwide (Simmons and Heinrich, 1980; Simmons et al., 1987),  $La_N/Yb_N$  ratios of approximately 10, and significant negative Eu anomalies (Figs. 3A and 4). One sample, WL4-1 (Table 1), has somewhat lower  $Fe_2O_3$ , Zr, Y, Nb, Hf, U, and HREE, but appears mineralogically similar to the other three. This sample was not included in the average composition of the granite used in our bulk pegmatite model described below.

### Pegmatite Wall Zone

The 5- to 15-cm-thick wall zone consists of a relatively fine-grained graphic intergrowth of quartz and perthitic microcline with biotite and occasional zircon grains. Quartz content is greater and biotite content is lower than in the granite, and Na-plagioclase occurs only in the perthite and not as independent grains. Fe-oxides and fluorite are absent.

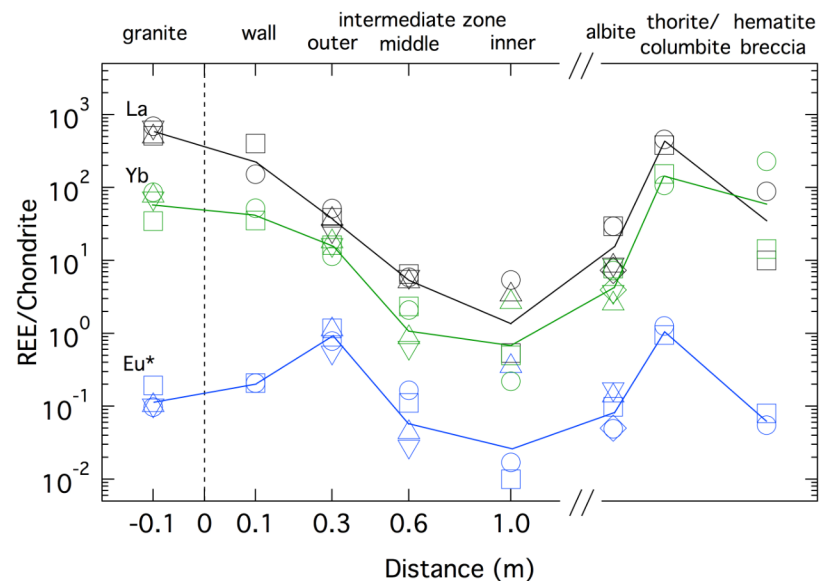


**Figure 4. Spatial trends in LREE and HREE content, represented by  $La_N$  and  $Yb_N$ , across the different pegmatite zones from the granite to the core region, with continuous REE depletion. This contrasts with the increase in REE in the albite, and, notably, thorite, columbite, and hematite breccia in the pods in the “replacement zone” at the IIZ-quartz core boundary, with a trend toward higher HREE, offset by the LREE minerals fluorite and bastnäsite (Fig. 3C). Note the absence of the Eu\* anomaly in the OIZ. Different symbols (squares, circles, triangles) represent specific individual samples from the tables.**

Samples of the wall zone (Figs. 3B and 4; Table 2) have compositions similar to the granite host (Table 1), but with slightly lower total REE contents, a feature also noted for this zone in South Platte pegmatites (Simmons and Heinrich, 1980; Simmons et al., 1987). This depletion in total REE relative to the granite host possibly reflects the greater abundance of quartz, and lower abundance of feldspars compared to the granite. The  $La_N/Yb_N$  ratios of these samples vary from 10 to 5. The negative Eu anomaly for the wall zone is also less pronounced than for the granite, possibly due to the higher proportion of potassium feldspar, which relative to plagioclase concentrates Eu as it crystallizes. In this zone plagioclase only occurs in the microcline-perthite, not as a primary crystallization phase. This zone also has lower Zr, Y, Th, and U contents than the granite (Table 2), which is reflected mineralogically in the scarcity and small size of zircon crystals.

### Pegmatite Intermediate Zone

In the outer intermediate zone (OIZ), the graphic intergrowth of quartz and perthitic microcline be-

comes coarser and can be observed macroscopically, biotite occurs in decreased abundance as scattered large plates, and zircon is absent. Further inward toward the core of the pegmatite and away from the contact with the granite, this ~20-cm-wide OIZ changes to a middle intermediate zone (MIZ) of even coarser microcline-perthite without any biotite. There is then an inner intermediate zone (IIZ) of coarse microcline-perthite without quartz and the appearance of small euhedral laths of albite. These appear to have crystallized directly from the pegmatite parental magma.

Four samples from the OIZ (Table 2) have lower  $Fe_2O_3^{total}$  and  $TiO_2$  than the granite, reflecting the lower concentration of biotite, and significantly lower REE contents, with lower  $La_N/Yb_N$  ratios between 2 and 3. These samples lack a negative Eu anomaly (Figs. 3B and 4). The lack of a negative Eu anomaly in this zone may reflect the fact that potassium feldspar, which was the dominant feldspar crystallizing from the pegmatite parental magma prior to evolving into perthite during cooling, concentrates Eu relative to other REE. Ba, Sr, Zr, Nb, Th, Hf, and U contents are also lower than in ei-

ther the granite or wall zone (Table 2). Four samples from the MIZ (Table 2) have  $La_N/Yb_N$  ratios between 1 and 5. Three samples from the IIZ (Table 2) have significantly lower REE concentrations despite the absence of quartz. Two of these samples have  $La_N/Yb_N$  of ~1.

### Albite and Hematite-rich Pods

Local segregations between the perthitic microcline-rich intermediate zone and the quartz-rich core of the pegmatite are characterized by white-bladed albite (var. ‘cleavelandite’). These pods are more heterogeneous than the intermediate zone, as indicated by the chemical analysis of 10 samples from this zone (Table 3). They contain (1) areas of albite intergrown with quartz (samples WL5-1 and WL5-5); (2) areas of almost pure albite (WL5-4A, WL5-4B, and WL7-1); (3) albite with accessory thorite (WL5-2) and/or columbite (WL5-3), as well as pockets of albite and hematite (WL4-6A and WL4-6B); and (4) breccias dominated by hematite (WL6-1). Simmons and Heinrich (1980) and Simmons et al. (1987) suggested that similar associations observed in South

**Table 1. Compositions of pink potassic series Pikes Peak granite samples from the area around the Wellington Lake pegmatite in comparison with previous published analyses from Smith et al. (1999).**

PP granites	Wellington Lake pegmatite area				Smith et al. (1999)			
Sample No.	WL4-1	WL8-1	WL8-2	WL19	GM7-BG	WP33BG	85BP4	SPDIR
Ox. Wt. %								
SiO <sub>2</sub>	73.73	76.43	75.55	73.63	70.41	73.13	71.6	72.5
TiO <sub>2</sub>	0.10	0.21	0.17	0.22	0.52	0.30	0.27	0.27
Al <sub>2</sub> O <sub>3</sub>	12.88	11.12	11.74	12.53	13.79	12.63	12.70	12.60
Fe <sub>2</sub> O <sub>3</sub>	1.70	2.65	2.29	2.52	3.75	3.18	0.65	0.58
MnO	<0.01	0.06	0.03	<0.01	0.08	0.08	0.07	0.06
MgO	0.03	0.02	0.02	0.03	0.55	0.14	0.11	0.12
CaO	1.17	0.68	0.99	0.89	1.57	1.03	1.14	0.98
Na <sub>2</sub> O	2.98	2.78	2.99	3.14	3.37	3.21	3.24	3.19
K <sub>2</sub> O	6.14	5.20	5.39	5.69	5.35	5.55	5.62	5.58
P <sub>2</sub> O <sub>5</sub>	<0.01	0.01	<0.01	<0.01	0.19	0.03	0.02	0.02
LOI	1.10	0.60	0.60	1.10				
<b>Sum</b>	<b>99.85</b>	<b>99.75</b>	<b>99.77</b>	<b>99.74</b>	<b>99.58</b>	<b>99.28</b>	<b>95.42</b>	<b>95.9</b>
<b>PPM</b>								
Ga	23.6	21.1	19.9	21.9				
Cs	1.1	2.2	1.6	2.2				
Ba	144	202	180	249	1208	529	450	450
Rb	222	254	225	254	210	210	225	209
Sr	19.6	15.9	17.6	20.3	173	67	47	55
Zr	103	637	436	511	557			
Y	55.2	127	125	139	718	92.2	94	69
Sn	2	6	4	7				
Nb	42.7	61.6	46.2	60.1			20	23
Ta	4.0	4.4	2.7	4.0	3.8	3.5		
Th	30.6	27.4	33.4	35.2	32	30	34	32
Hf	4.0	21.2	14.6	16.2				
U	3.9	6.7	5.0	7.4	3.3	3.3		
<b>REE</b>								
La	122	118	158	165	114	172	200	180
Ce	247	269	315	353	216	323	370	340
Pr	26.6	29.9	38.0	41.6				
Nd	88.6	112	137	151	90	135	153	156
Sm	13.5	22.7	26.6	28.4	15.8	23.6	23.6	28
Eu	0.78	0.75	0.86	0.89	2.3	1.3		
Gd	10.5	21.2	23.3	26.5				
Tb	1.61	3.43	3.61	4.65	2.1	3.1		
Dy	9.34	22.7	22.9	26.8				
Ho	1.82	4.43	4.30	5.56				
Er	5.23	13.0	12.4	15.0				
Tm	0.83	2.01	1.84	2.19				
Yb	5.59	12.4	11.5	13.8	8.74	10.2	10	7
Lu	0.90	1.80	1.68	2.00	1.31	1.48		

Platte pegmatites formed from volatile-rich fluids that developed during a late stage of crystallization. They referred to these associations as a “replacement zone.” In the Wellington Lake pegmatite, although low temperature magmatic or meteoric fluids might have resulted in the formation of hematite from magnetite, the bladed albite laths are fresh and unaltered. We see no textural evidence that these laths have resulted from secondary replacement processes and consider them as primary magmatic features. Together, these so-called “replacement zone” associations com-

prise only ~1 vol. % of the pegmatite. The albite-rich zones have  $La_N/Yb_N$  ranging from 1 to 10, while the hematite-rich samples have  $La_N/Yb_N < 1$  (Figs. 3C and 4).

### Pegmatite Core

In the roof of the quartz core, in contact with the intermediate zone, an ~0.8 m × 0.5 m × 0.4 m cavity was discovered during the investigation. The cavity is formed by large intergrown microcline-perthite and quartz crystals, and

**Table 2. Compositions of samples from the wall zone, and the outer, middle, and inner intermediate zones of the Wellington Lake pegmatite.**

Sample No. Ox. Wt. %	Wall Zone		Outer Intermediate Zone (OIZ)				Middle Intermediate Zone (MIZ)				Inner Intermediate Zone (IIZ)		
	WL4-2B	WL4-3	WL4-4	WL8-4A	WL8-6A	WL4-5	WL9-6	WL9-5	WL9-4	WL9-3	WL9-2	WL9-1	WL6-3
SiO <sub>2</sub>	74.9	74.7	75.2	75.8	75.9	75.5	76.5	77.3	75.8	75.6	67.0	66.0	65.4
TiO <sub>2</sub>	0.16	0.09	0.02	0.02	0.02	<0.01	<0.01	<0.01	<0.01	<0.01	<0.01	<0.01	<0.01
Al <sub>2</sub> O <sub>3</sub>	12.5	12.9	13.3	13.3	13.1	13.2	13.1	12.9	13.6	13.6	18.4	18.9	18.5
Fe <sub>2</sub> O <sub>3</sub>	2.06	1.12	0.42	0.27	0.46	0.19	0.21	0.16	0.14	0.1	0.07	0.18	0.42
MnO	<0.01	<0.01	<0.01	<0.01	<0.01	<0.01	0.01	0.01	0.01	0.01	0.01	0.01	0.01
MgO	0.03	0.03	<0.01	<0.01	<0.01	<0.01	0.01	0.01	0.01	0.01	0.01	0.03	<0.01
CaO	0.63	0.87	0.35	0.3	0.16	0.16	0.11	0.11	0.06	0.05	0.07	0.04	0.02
Na <sub>2</sub> O	3.21	3.00	3.42	3.15	2.92	2.77	2.89	2.85	2.91	2.70	4.70	2.33	2.84
K <sub>2</sub> O	5.60	6.29	6.46	6.66	6.89	7.54	7.27	6.99	7.58	7.72	9.33	12.8	12.4
P <sub>2</sub> O <sub>5</sub>	<0.01	<0.01	<0.01	<0.01	<0.01	<0.01	<0.01	<0.01	<0.01	<0.01	<0.01	<0.01	<0.01
LOI	0.7	0.8	0.7	0.4	0.5	0.5	0.39	0.41	0.44	0.4	0.49	0.65	0.5
Sum	99.8	99.8	99.9	100.0	100.0	99.9	100.5	100.7	100.6	100.2	100.0	100.9	100.0
PPM													
Ga	21	23	21	25	22	21	24	22	25	26	42	46	34
Cs	2.6	0.9	1.7	1.3	0.7	1.5	0.7	1.0	1.2	2.0	2.9	3.9	2.7
Ba	288	102	86	69	86	124	8	10	9	41	68	196	202
Rb	231	227	322	247	254	496	497	455	539	760	822	>1000	973
Sr	21.9	15.8	10.4	9.8	9.6	3.6	5.0	4.0	4.0	7.0	8.0	11.0	2.8
Zr	377	139	19.4	31.7	33.8	21.6	17.0	16.0	12.0	9.0	2.0	4.0	1.4
Y	75.8	52.0	15.3	14.8	13.3	15.9	17.0	16.4	4.9	2.8	0.8	3.7	2.5
Sn	6	3	3	4	2	1	2	3	3	2	2	5	5
Nb	39.9	41.1	9.5	15.2	15.9	16.0	7.8	7.4	5.9	4.0	0.6	1.1	11.2
Th	13.2	27.7	4.5	7.4	6.8	4.2	5.6	3.6	2.0	1.5	0.14	0.05	1.0
Hf	12.5	6.1	1.0	1.9	2.6	1.9	1.3	1.2	0.9	1.0	<0.1	<0.1	<0.1
U	3.7	4.3	1.6	1.7	1.9	1.6	1.1	1.0	0.6	0.5	0.1	0.44	2.1
<b>REE</b>													
La	36.2	94.7	12.2	9.10	8.80	6.00	5.87	6.50	5.13	6.01	5.39	0.54	0.80
Ce	86.1	197	19.6	18.8	22.2	10.8	7.53	8.22	6.76	7.73	6.04	0.85	1.40
Pr	11.6	21.1	2.37	1.41	1.43	1.21	0.91	0.97	0.54	0.66	0.30	0.11	0.20
Nd	48.6	70.5	8.20	5.20	5.30	4.50	3.33	3.71	1.70	1.73	0.55	0.35	0.80
Sm	11.5	11.5	1.71	1.30	1.21	1.18	1.04	0.93	0.37	0.35	0.11	0.12	0.24
Eu	0.80	0.72	0.46	0.51	0.47	0.22	0.17	0.11	0.04	0.03	0.02	0.01	<0.02
Gd	11.7	9.10	1.83	1.33	1.32	1.24	1.19	1.22	0.35	0.30	0.10	0.16	0.26
Tb	2.08	1.47	0.35	0.29	0.29	0.28	0.27	0.26	0.08	0.07	0.02	0.05	0.08
Dy	12.4	8.57	2.26	2.34	2.41	2.37	1.86	1.94	0.64	0.44	0.17	0.43	0.55
Ho	2.69	1.73	0.50	0.52	0.55	0.52	0.41	0.44	0.16	0.10	0.04	0.11	0.13
Er	8.11	5.23	1.50	1.92	2.06	1.95	1.43	1.55	0.58	0.38	0.12	0.38	0.35
Tm	1.27	0.88	0.26	0.35	0.39	0.35	0.27	0.29	0.11	0.07	0.03	0.07	0.07
Yb	8.42	5.67	1.84	2.61	2.93	2.63	2.08	2.33	0.88	0.64	0.22	0.50	0.43
Lu	1.31	0.87	0.30	0.42	0.45	0.41	0.34	0.39	0.16	0.12	0.05	0.09	0.06

filled with elongated euhedral smoky quartz crystals up to 15 cm long, albite-hematite breccia fragments, yellow-green clay, and hematite dust. In addition, ~30 euhedral 0.5 cm to 4 cm in size fluocerite crystals, with bastnäsite overgrowths, were found concentrated at the bottom of the cavity. The fluocerite has  $La_N/Yb_N \sim 1,000$  (Fig. 3C).

### REE Mineralogy

REE and HFSE minerals found in the pegmatite include columbite, zircon, thorite, fluocerite, and bastnäsite. Columbite is found both as well-formed crystals up to 6 cm in association with albite and microcline as well as subhedral masses associated with biotite. In the biotite, columbite is associated with secondary uranium minerals that occur as coating and thin fracture fillings. Nodules of zircon and thorite up to 5 cm in size are also associated with the biotite, locally with cassiterite inclusions of 10s of mm in size. The

zircon-thorite ('cyrtolite') is also found locally in small pits on the surface of large euhedral quartz crystals.

Most notable for the pegmatite are the well-developed tabular crystals of fluocerite-(Ce) [(REE)F<sub>3</sub>], which are overgrown by bastnäsite-(Ce) [(REE)CO<sub>3</sub>F], as shown in Fig. 5A. Such fluocerite-bastnäsite crystals were first described from the Pikes Peak granite batholith (Cheyenne Canyon; Mount Rosa intrusive center) by Allen and Comstock (1880), who gave the fluocerite cores a new name, 'tysonite,' after its discoverer, S. T. Tyson. Allen and Comstock were apparently not aware of the previous work of Berzelius (1818), who described a new mineral from granitic pegmatites at Finnbo and Broddbo near Falun, Sweden, as "*Neutralt Fluss-spatsyrat Cerium*," later named 'fluocerite' by Haidinger (1845). Geijer (1921) restudied the type material from Sweden, recognizing that the Swedish fluocerite is identical with tysonite, although the name tysonite can be found in the literature up to 1965 (Sverdrup et al., 1965).

**Table 3. Compositions of different albite-rich pods occurring at the contact of the intermediate zone and the core zone of the pegmatite.**

Sample No. Ox. Wt. %	Albite (cleavelandite) +/- quartz					+ Thorite	+ Columbite	+ Hematite		
	WL5-1	WL5-5	WL5-4A	WL5-4B	WL7-1	WL5-2	WL5-3	WL4-6B	WL4-6A	WL6-1
SiO <sub>2</sub>	74.7	77.4	68.1	67.6	65.3	66.5	63.7	47.1	50.1	7.93
TiO <sub>2</sub>	<0.01	<0.01	<0.01	<0.01	0.03	0.01	0.06	0.27	0.03	<0.01
Al <sub>2</sub> O <sub>3</sub>	15.5	13.9	19.8	19.9	19.8	19.9	18.9	17.1	15.7	1.60
Fe <sub>2</sub> O <sub>3</sub>	0.36	0.17	<0.04	0.05	2.20	0.52	2.59	19.7	19.5	76.7
MnO	<0.01	<0.01	<0.01	<0.01	<0.01	<0.01	<0.01	<0.01	<0.01	<0.01
MgO	<0.01	<0.01	<0.01	<0.01	0.04	0.01	0.04	0.30	0.17	<0.01
CaO	0.28	0.24	0.14	0.33	0.31	0.36	0.44	1.61	2.10	0.05
Na <sub>2</sub> O	8.41	7.67	11.44	11.48	10.46	10.93	9.88	3.91	6.96	0.05
K <sub>2</sub> O	0.26	0.18	0.13	0.15	0.55	0.37	0.34	3.23	0.66	0.12
P <sub>2</sub> O <sub>5</sub>	<0.01	<0.01	<0.01	<0.01	<0.01	<0.01	0.01	<0.01	<0.01	<0.01
LOI	0.4	0.4	0.3	0.4	1.2	0.7	1.8	6.2	4.6	13.4
Sum	99.9	99.9	100.0	100.0	100.0	99.4	97.8	99.5	99.9	99.8
PPM										
Ga	34.5	31.4	70.6	64.2	64.2	50.5	46.9	84.5	44.4	3.0
Cs	0.3	0.2	0.2	0.2	1.7	0.5	1.6	9.7	1.4	0.3
Ba	5	4	2	2	4	12	21	34	9	4
Rb	14.5	10.9	2.1	4.6	166	30.4	37.9	627	92.8	11.1
Sr	1.6	1.2	2.3	1.5	4.1	6.0	7.2	19.1	14.5	2.4
Zr	6.0	5.7	2.4	2.0	3.2	810	117	1821	124	4.0
Y	4.5	7.1	1.7	4.0	21.1	412	557	333	187	136
Sn	4	2	1	2	15	27	163	76	41	2
Nb	58.1	22.5	10.5	15.1	19.4	179	6512	272	263	9.3
Ta	0.9	6.9	6.1	3.9	9.0	9.6	1894	28.4	3.9	0.6
Th	3.8	1.2	1.0	2.6	5.5	138	1062	543	47	1.9
Hf	0.7	0.5	0.2	0.1	0.4	100	9.8	101	7.1	0.2
U	2.2	1.9	2.1	5.4	5.1	36.6	1836	47.4	14.5	178
<u>REE</u>										
La	7.00	3.90	2.00	2.10	7.30	459	384	26.8	15.4	10.0
Ce	18.1	7.50	5.60	6.10	19.2	1381	995	35.7	19.0	11.6
Pr	1.64	0.93	0.64	0.61	2.45	169	133	7.75	4.35	3.25
Nd	4.90	2.40	1.00	1.00	8.30	563	460	31.0	17.6	12.6
Sm	1.31	0.56	0.48	0.35	2.53	140	113	9.87	5.06	4.41
Eu	<0.02	<0.02	<0.02	<0.02	0.05	1.26	0.95	0.28	0.11	0.08
Gd	1.11	0.68	0.37	0.35	2.94	118	98.7	20.9	8.16	8.27
Tb	0.24	0.17	0.08	0.09	0.65	19.3	23.1	6.63	2.03	2.23
Dy	1.49	1.19	0.39	0.63	4.21	98.3	164	54.0	15.1	17.4
Ho	0.28	0.28	0.10	0.14	0.97	19.1	36.5	13.5	3.90	4.41
Er	0.85	0.95	0.31	0.45	3.11	62.4	120	46.9	12.6	14.1
Tm	0.16	0.17	0.06	0.09	0.54	13.2	22.3	8.42	2.09	2.23
Yb	1.17	1.25	0.41	0.60	3.93	107	153	59.9	13.8	14.3
Lu	0.19	0.20	0.06	0.10	0.61	18.0	21.1	9.99	2.04	2.28

Fluocerite, while overall uncommon in Pikes Peak pegmatites, has been reported locally in abundance, notably in the Black Cloud, Little Patsy, and Mount Rosa area pegmatites, some with, some without bastnäsite association. Additional descriptions of fluocerite crystals overgrown by bastnäsite in Colorado were made by Hidden (1891) from the Crystal Peak area, Hillebrand (1899), and Glass and Smalley (1945). The exact structural relationship between the two minerals was only recently confirmed from crystallographic and high-resolution TEM analysis as an epitaxial growth along the crystallographic *c*-axis associated with the hexagonal symmetry, with close lattice match (Müller et al., 2011; our Fig. 5B). In addition to the epitaxial overgrowth relationship, bastnäsite replacement of fluocerite (typically on crystal or grain margins or along cleavage planes) has been noted by several authors (Lahti and Suominen, 1988; Beukes et al., 1991).

Polarization resolved micro-Raman spectroscopy, with vibrational modes characteristic for the two mineral species and their spatial invariance across the crystal (Fig. 5C), confirms the single crystal nature of both the fluocerite and bastnäsite in the Wellington Lake pegmatite. Both fluocerite and bastnäsite have space group  $P6_3/mcm$  and corresponding symmetry point group  $D_{6h}$ . Based on the Raman active modes and the respective Raman tensors ( $A_{1g}$ ,  $E_{1g}$ , and  $E_{2g}$ ), the crystallographic orientation was determined through choice of input and output polarization (H and V respective to the *c*-axis) (Kuzmany, 2009). This indicates the parallel orientation of the (0001) crystal planes of the fluocerite core and bastnäsite. Together with the bastnäsite primarily grown on the (0001) crystal plane of fluocerite, of even thickness and a straight phase boundary (see also Fig. 6A and B showing a region of the only major disturbance of

**Table 4. Electron microprobe analyses of a euhedral fluocerite and the bastnäsite overgrowth on this crystal, in comparison with a bulk ICP-MS analysis of another fluocerite crystal from the same mineralized pocket.**

Sample	Bastnäsite				Fluocerite	
	Low Gd	High Gd	High Ce	average	average	ICP-MS
Ox. Wt. %						
ThO <sub>2</sub>	-	0.53	0.9	0.38	1.09	1.07
Y <sub>2</sub> O <sub>3</sub>	-	0.58	0.2	0.29	0.46	0.95
La <sub>2</sub> O <sub>3</sub>	14.87	11.88	17.72	15.52	21.35	19.82
Ce <sub>2</sub> O <sub>3</sub>	35.86	32.01	36.33	34.72	41.9	36.08
Pr <sub>2</sub> O <sub>3</sub>	3.83	3.83	3.22	3.51	3.86	3.77
Nd <sub>2</sub> O <sub>3</sub>	14.3	16.24	10.84	13.33	14.21	11.66
Sm <sub>2</sub> O <sub>3</sub>	2.1	4.09	2.02	2.48	1.87	1.68
Eu <sub>2</sub> O <sub>3</sub>	-	-	-	-	-	0.03
Gd <sub>2</sub> O <sub>3</sub>	0.6	2.14	1.04	1.19	0.79	0.67
Tb <sub>2</sub> O <sub>3</sub>	-	0.14	0.12	0.12	0.07	0.07
Dy <sub>2</sub> O <sub>3</sub>	-	0.31	-	0.16	0.17	0.24
Yb <sub>2</sub> O <sub>3</sub>	-	-	-	-	-	0.02
MgO	-	-	-	0	0.01	0.01
CaO	-	0	-	0	0.25	0.86
F	8.77	8.35	8.6	8.62	32.64	19.9
CO <sub>2</sub>	19.07	19.07	19.32	19.1	-	-
O=F	-3.69	-3.52	-3.62	-3.63	-13.74	-
Total	95.71	95.65	96.69	95.79	104.93	96.82
apfu:						
Th	-	0.005	0.002	0.003	0.008	0.008
Y	-	0.012	0.007	0.006	0.008	0.018
La	0.211	0.168	0.238	0.219	0.250	0.255
Ce	0.504	0.45	0.507	0.487	0.488	0.461
Pr	0.054	0.054	0.046	0.049	0.045	0.048
Nd	0.196	0.223	0.168	0.183	0.161	0.145
Sm	0.028	0.054	0.021	0.033	0.020	0.020
Gd	0.008	0.027	0.009	0.015	0.008	0.008
Eu	-	-	-	-	-	<0.001
Tb	-	0.002	0.001	0.001	0.001	0.001
Dy	-	0.004	-	0.002	0.002	0.003
Yb	-	-	-	-	-	<0.001
Mg	-	-	-	-	0.001	0.001
Ca	-	-	0.001	-	0.009	0.032
F	1.065	1.014	1.061	1.046	3.283	3 (fixed)
C <sub>fixed</sub>	1	1	1	1		
O <sub>fixed</sub>	3	3	3	3		
Total	6.065	6.013	6.061	6.045	4.284	4 (fixed)

the interface), this suggests epitaxial overgrowth similar to the observations of Müller et al. (2011), rather than pseudomorphic replacement.

Electron microprobe analyses (Table 4) of the area indicated in Fig. 5A (white dashed box) reveals both a similar and high REE content of both minerals, and a chemically homogeneous fluocerite core with the empirical formula  $(La_{0.25}Ce_{0.49}Pr_{0.05}Nd_{0.16}Sm_{0.02}Gd_{0.01}HREE_{0.01})F_3$ . For comparison, a bulk ICP-MS analysis was performed on a different fluocerite crystal that yielded an average composition of  $(La_{0.23}Ce_{0.42}Pr_{0.04}Nd_{0.13}Sm_{0.02}Gd_{0.01}HREE_{0.01}Ca_{0.03})F_3$ . This is in good agreement with the EMP results and confirms the high  $La_N/Yb_N \sim 1,000$  of the fluocerite. In contrast, the bastnäsite is zoned with respect to REE and exhibits linear bands of enrichment in Gd, Sm, and Y perpendicular to the c-axis (Fig. 6C–E). An average empirical formula of  $La_{0.20}Ce_{0.44}Pr_{0.05}Nd_{0.21}Sm_{0.04}Gd_{0.03}HREE_{0.02})CO_3F$  is derived for the bastnäsite.

### Neodymium Isotopes

Neodymium isotopic compositions (Table 5) were determined for a fluocerite crystal from the Wellington Lake pegmatite and for two bulk samples of REE mineral-rich pods from the White Cloud pegmatite, a classic NYF-type pegmatite located to the east in the central South Platte district (Fig. 1). The isotopic ratios of these samples plot close to a 1.08 Ga isochron (Fig. 7A), as do samples from the PPG (Smith et al., 1999). The initial  $\epsilon_{Nd}$  values at 1.08 Ga for the Wellington Lake pegmatite fluocerite is -1.6, and for the REE mineral-rich pods from the White Cloud pegmatite are -2.0 and -2.1 (Fig. 7B). These values fall within the range of -0.2 to -2.7 determined for the potassic series rocks from the PPG. They are consistent with the formation of the potassic series rocks of the PPG by either melting of tonalitic crustal rocks (Smith et al., 1999; Frost and Frost, 2011) or a more complex history of crystallization of man-

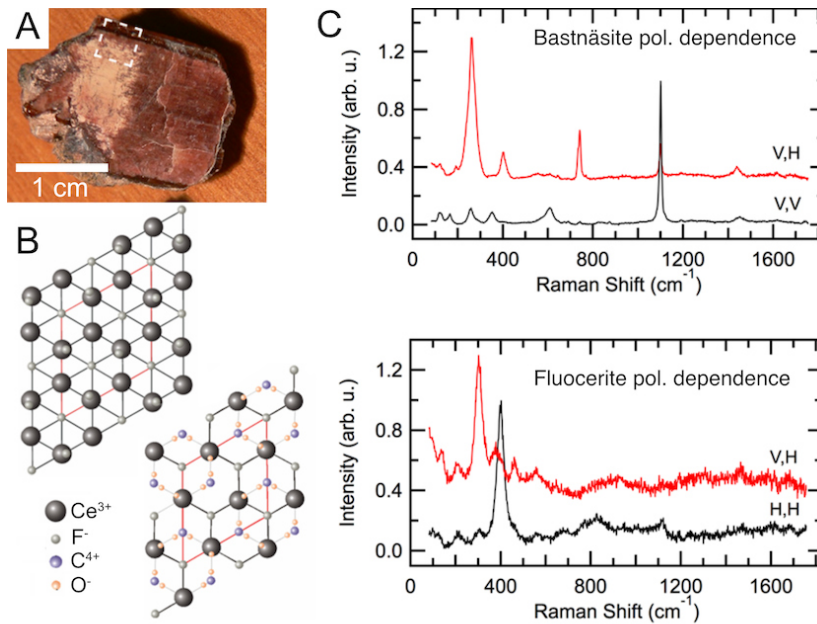


**Figure 5.** *A*, Cross section of typical fluocerite crystal (light to darker brown bulk) with mm to sub-mm thick bastnäsite overgrowth (dark rind). *B*, Lattice structure of fluocerite (top) and bastnäsite (bottom) of the (0001) crystal plane (after Müller et al., 2011). *C*, Polarization resolved Raman spectra and selection rules indicate epitaxial overgrowth facilitated by lattice match.

tle-derived basaltic magma combined with crustal assimilation (DePaolo, 1981; Guitreau et al., 2016).

## FLUID INCLUSIONS

Fluid inclusions in pegmatite core-zone quartz of three different generations were analyzed by microthermometry. The quartz samples include one large crystal (W-26) from the center of the core, which had no clear terminations, a second large crystal (W-3) from along the contact between the core and microcline of the IIZ, and a third doubly terminated euhedral crystal (W-29) spatially associated with the fluocerite and bastnäsite mineralization.

Inclusions are abundant in all three samples (Fig. 8). They include both clearly secondary inclusions trapped along fractures, and possible primary inclusions randomly distributed or parallel to crystal growth planes defined by crystal faces. Four types of inclusions were identified: (1) type A two-phase (> 80% liquid, and < 20% vapor) liquid-rich inclusions (Fig. 8B); (2) type B two-phase (> 60% vapor, and < 40% liquid) vapor-rich inclusions; (3) rare type C inclu-

sions containing transparent cubic crystals we interpret as halite (Fig. 8C); and (4) type D CO<sub>2</sub>-bearing inclusions (Fig. 8D). Types A, B, and C had no visual CO<sub>2</sub> bubbles at room temperature. This suggests the presence of an aqueous H<sub>2</sub>O-NaCl fluid with little or no CO<sub>2</sub>, and a distinct H<sub>2</sub>O-CO<sub>2</sub> fluid. Quartz crystals W-26 from the center of the core and W-3 from the edge of the core had all four types of inclusions, whereas sample W-29, associated with the REE mineralization, had only type A and type D inclusions.

The thermometric behavior of possible primary inclusions belonging to the three CO<sub>2</sub>-free populations (types A, B, and C) suggests, by eutectic points very close to -21°C, that most of these inclusions trapped solutions of the H<sub>2</sub>O-NaCl-system. A small group of these inclusions has slightly lower eutectic temperatures, between -22 and -24°C, indicative of other cations in solution, possibly K<sup>+</sup>. The absence of any low eutectic point (-50°C) inclusions precludes the presence of CaCl<sub>2</sub> in the solutions. The majority of inclusions are liquid-rich type A of intermediate salinities between 10 and 16 wt. % NaCl equiva-

lent, which homogenize between 119 and 196°C (Fig. 8A). In sample W-26, from the center of the core, type B vapor-rich inclusions, with > 60% vapor, homogenize at 340 to 360°C, and have salinities of 3 to 6 wt. % NaCl (Fig. 8A). In addition, a few of the relatively rare halite-bearing type C fluid inclusions, with salinities around 28 wt. % NaCl and homogenization temperatures of 320 to 380°C, were measured in sample W-26. Both types B and C also occurred in sample W-3 from the edge of the core, but could not be measured in this sample. A pressure correction of 1,500 bar, equivalent to a crystallization depth of 5 km as estimated by Simmons and Heinrich (1980) for the depth of solidification of the PPG, indicates a maximum entrapment temperature of ~490°C for the halite-bearing type C inclusions in quartz crystal W-26.

## DISCUSSION

### Pegmatite Bulk Chemical Composition

The mineralogy and chemistry of the pegmatite appears to reflect a series of primary magmatic processes, as indicated by the absence of any evidence of major secondary hydrothermal or weathering processes in either the pegmatite or surrounding host granite. Thus, we see no indication of secondary exchange of elements with the larger volume of surrounding Pikes Peak granite. Minor hydrous sec-

**Table 5. Nd-isotope analysis of a fluocerite crystal from the Wellington Lake pegmatite and REE-mineral rich segregations from the White Cloud pegmatite in the South Platte district.**

Sample	Sm (ppm) <sup>a</sup>	Nd (ppm) <sup>a</sup>	<sup>147</sup> Sm/ <sup>144</sup> Nd	<sup>143</sup> Nd/ <sup>144</sup> Nd <sup>b</sup> (m)	$\epsilon_{\text{Nd}}(0)^c$	$\epsilon_{\text{Nd}}(T)^c$
Wellington Lake fluocerite	2,842 ± 1	20,331 ± 2	0.0846	0.51176 ± 0.00001	-17.2	-1.6
White Cloud WhC R3A	7,242 ± 1	24,209 ± 4	0.1810	0.51242 ± 0.00001	-4.3	-2.1
White Cloud WhC R4A	7,605 ± 3	26,050 ± 4	0.1766	0.51239 ± 0.00001	-4.8	-2.0

Total procedural blanks averaged ~100 pg for Nd during study period.

Analyses were dynamic mode, three-collector measurements. Thirty-two measurements of the La Jolla Nd Standard during the study period yielded a mean <sup>143</sup>Nd/<sup>144</sup>Nd = 0.511840 ± 1 (2-σ mean).

$\epsilon_{\text{Nd}}(0)$  are measured (present-day) values, initial  $\epsilon_{\text{Nd}}$  calculated at T = 1080 Ma.

<sup>a</sup> Isotope dilution concentration determinations accurate to 0.5% for Sm and Nd.

<sup>b</sup> Measured <sup>143</sup>Nd/<sup>144</sup>Nd normalized to <sup>146</sup>Nd/<sup>144</sup>Nd = 0.7219.

<sup>c</sup>  $\epsilon_{\text{Nd}}$  values calculated using a present-day <sup>143</sup>Nd/<sup>144</sup>Nd (CHUR) = 0.512638.

ondary uranium mineralization on columbite, and host rock alteration around the cyrtolite, suggest some late-stage alteration possibly associated with metamictization. The pods of albite—in the form of euhedral crystal aggregates intergrown with quartz, hematite, columbite, zircon, and thorite—are similar to the associations in the “replacement” zones of the South Platte pegmatite district, which Simmons and Heinrich (1975, 1980) and Simmons et al. (1987) suggest were formed from volatile-rich pegmatite fluids developed during a late stage of crystallization. Alternatively, Černý et al. (1999) suggested that hematite in the nearby McGuire pegmatite may have formed by oxidation of magnetite by subsolidus pegmatite fluids at high  $f_{\text{O}_2}$ . However, it remains unclear why the Wellington Lake and other South Platte pegmatites hosted in the magnetite-bearing ferroan PPG contain hematite.

We have estimated the bulk composition of the pegmatite, for comparison with the host granite. The whole-rock analyses of different pegmatite zones allow for an estimate of the average composition of each zone (Data Supplement 1 [DS 1]). From mapping the pegmatite to the best extent possible within the constraints of external and internal exposure (Fig. 2), and translating the spheroidal shape into a sphere, the volumes of the different zones were obtained and converted to masses based on measured densities of their constituent mineral phases (Data Supplement 2 [DS 2]). For the thorite, columbite, and hematite bearing zones, as well as the fluocerite, total masses were estimated based on the field observations of their total modal abundances, which are small. Overall, with a 5% void space in the quartz core, the total pegmatite mass is just slightly lower than the mass of granite of equivalent volume. This is consistent with the pegmatite being derived from the magma that formed the granite, but enriched in water, which after crystallization escaped from the system.

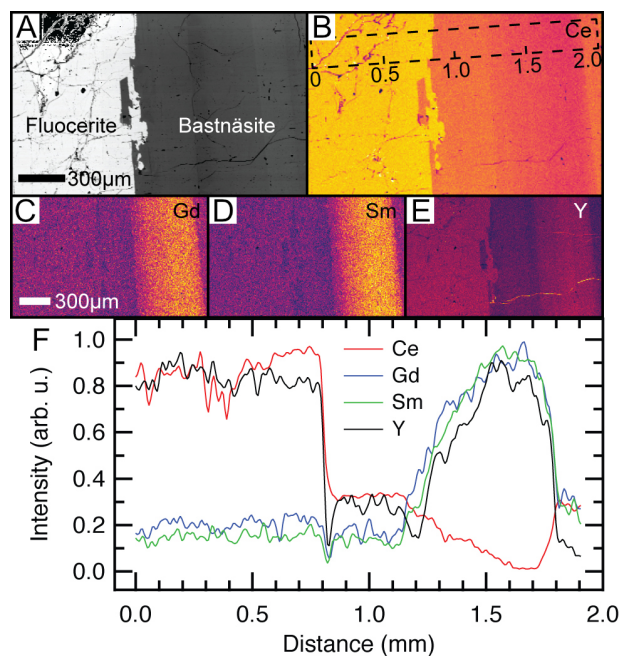


**Figure 6. A, Backscattered electron image of fluocerite-bastnäsite interface. B–E, Microprobe X-ray element maps for Ce, Gd, Sm, and Y (Figs. B–E, respectively) highlighting mostly spatially homogeneous fluocerite composition, yet concentric zoning of the bastnäsite overgrowth. F, Integrated X-ray intensity (arbitrary units) transect of REE variation of the area indicated in Figure 6B, with anticorrelation of LREE (Ce) and HREE (Gd, Sm, and Y).**

With the average compositions from DS 1 and estimated volumes for each zone from DS 2, the corresponding masses of the individual element oxides for each zone can be calculated. From their sum, the overall composition of the whole pegmatite can be obtained and compared to a granite

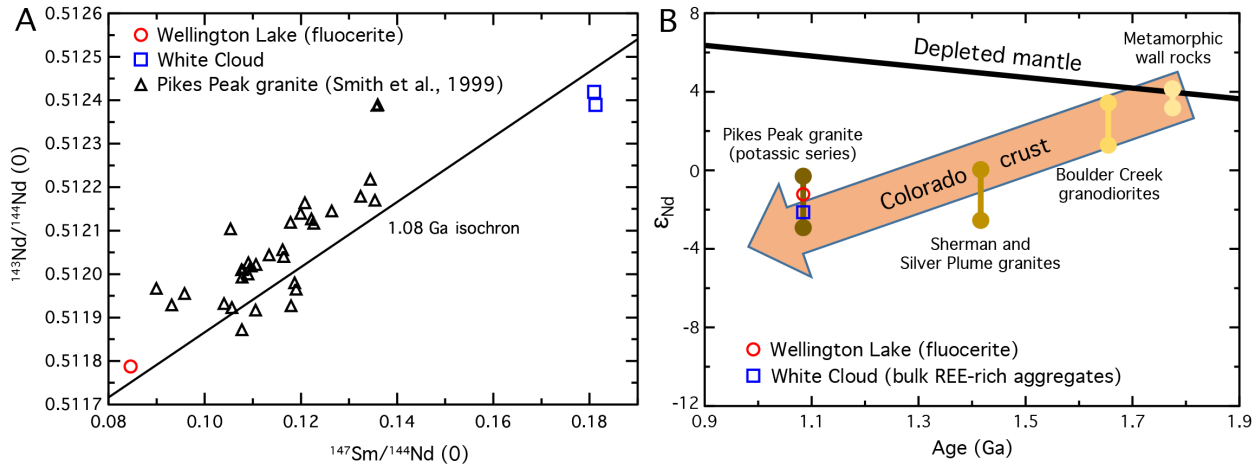


Figure 7. A, Measured Nd-isotopic ratios of fluocerite from the Wellington Lake pegmatite and REE-rich aggregates from the White Cloud pegmatite in comparison with bulk samples of Pikes Peak granite from Smith et al. (1999) compared to a 1.08 Ga isochron. B, Corresponding  $\epsilon_{\text{Nd}}$  versus age compared to the Proterozoic crustal rocks from Colorado, including the metamorphic basement, Boulder Creek granodiorites, Sherman and Silver Plume granites, and Pikes Peak granite (figure modified after Smith et al., 1999).

body of the same size (DS 2). The results of the comparison of model pegmatite composition and granite and their fractional difference for the different elements are shown in Table 6, and in graphical representation in Figure 9. Constrained by exposure, coarse-grained texture, and heterogeneity of the mineralized zones, this approach of pegmatite bulk composition analysis has its limitations. However, given the good exposure of this pegmatite and extrapolating from the even distribution of mineralized zones observed along the margin of the quartz core, we estimate an uncertainty of < 50% in the bulk pegmatite concentrations of the different trace elements, and much better for the estimation of the major elements. The lateral extent and top of the pegmatite are exposed and has been investigated well enough to conclude with good confidence that we have not missed any major element, REE- or HFSE-bearing phases. Although we were unable to probe the extent and mineralogy of the pegmatite at depth, the inward curvature of the pegmatite wall at the floor of the accessible cavities suggest a spheroidal shape. Further, from field observations of pegmatites in the South Platte district, it appears that the REE and HFSE mineral phases are generally concentrated in the upper regions of the pegmatites, making it unlikely that larger amounts of the associated elements have been missed.

The contents of Si, Al, K, and Na estimated for the Wellington Lake pegmatite are similar to that of Pikes Peak granite. Although the relative concentrations of these elements vary across the wall, intermediate, and core zones, the good agreement of the total content of these elements between the pegmatite and Pikes Peak granite indicate that the volume estimates, especially of the intermediate zone and quartz core, are approximately correct, with the implication

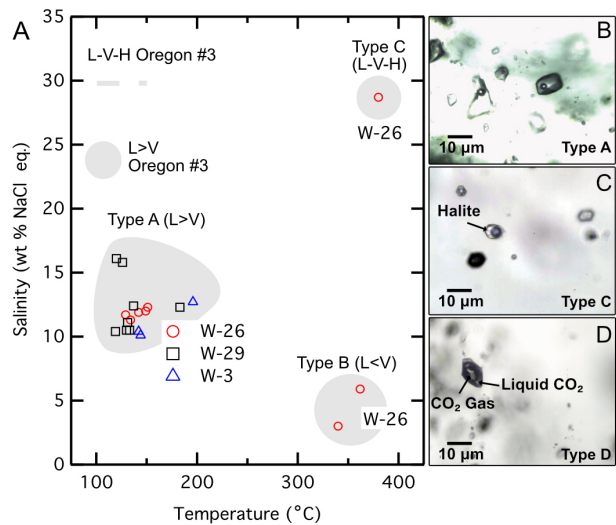
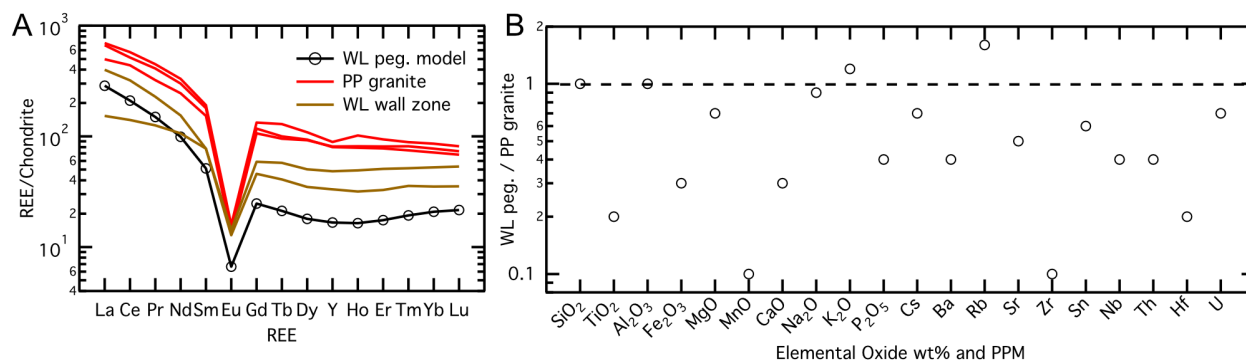


Figure 8. A, Temperature ( $^{\circ}\text{C}$ ) versus salinity (wt % NaCl equivalent) in fluid inclusions from three quartz crystals in the core of the Wellington pegmatite. B, Type A two-phase inclusions with > 80% liquid (L) and < 20% vapor (V) found in all three samples. C, Type C inclusions containing cubic crystals of what we interpret to be halite (H) found in quartz sample W-26 from the center of the core and the large quartz crystal W-3 from the edge of the core, but not in the doubly terminated crystal W-29 associated with the REE-mineralization. D, Type D  $\text{CO}_2$ -bearing inclusions found in all three quartz samples. Corresponding data of quartz-hosted secondary L-V and L-V-H inclusions from the Oregon #3 pegmatite are shown for comparison (Gagnon et al., 2004).



**Figure 9. A, The estimated bulk REE content of the Wellington Lake pegmatite. The pegmatite is overall depleted in REE compared to the Pikes Peak Granite (PPG). B, The estimated major and trace element content of the pegmatite normalized to that of the PPG. Although the pegmatite Si, Al, Na, and K approximates the PPG, the concentration of other elements differs significantly from that of the granite.**

that the parental pegmatite melt is principally derived from the PPG, consistent with the Nd-isotopic composition of fluocerite in the pegmatite.

However, and well within the uncertainty of the approach, the pegmatite overall is depleted in Fe, Mg, Mn, the HFSE (Ti, Hf, Zr, Th, Nb), along with P and Ca, as well as the alkaline earths Sr and Ba (Fig. 9). The pegmatite is further depleted in REE relative to the PPG, possibly slightly more for the HREE (Fig. 9). Therefore, despite the presence of the LREE minerals fluocerite and bastnäsite, the Wellington Lake pegmatite should not be considered as LREE-rich. We conclude that the fluocerite and bastnäsite crystallized from a small amount of LREE-enriched residual melt produced by the internal crystal-liquid fractionation processes associated with the solidification of the pegmatite. The early crystallization of the large volume of silicate minerals, with relatively low REE contents (Figs. 3 and 4), that form the wall, intermediate, and core zones of the pegmatite, combined with the progressive inward decrease in LREE/HREE in these zones, generated this LREE-enriched residual melt. Although the albite, hematite, thorite, and columbite pods reverse the inward trend and have higher REE than the IIZ (Figs. 3C and 4), the low LREE/HREE of the small volume of these pods further increased the LREE/HREE of the residual F, CO<sub>2</sub> and LREE-enriched melt from which the fluocerite and bastnäsite crystallized.

The depletion relative to the PPG in all REE for the Wellington Lake pegmatite contrasts with the reported total REE enrichment of a factor of ~10 relative to the host PPG for the Oregon #3 pegmatite in the South Platte district (Simmons and Heinrich, 1980). However, reanalyzing the original data, Simmons (personal communication, 2020) lowered the enrichment factor to at most 2.5, adding uncertainty whether the NYF-type pegmatites in the South Platte district are indeed REE enriched relative to the PPG. It has

been proposed that NYF-type pegmatites, such as those enriched in HREE and F in the central South Platte pegmatite district, would have developed their enhanced HREE concentration due to the high concentration of F in their parental melts (London, 2016). For the Wellington Lake pegmatite, which lacks significant F, the overall depletion compared to the PPG in all REE, in HREE relative to LREE, as well as HFSE, suggests that these elements were transferred from the PPG host into the pegmatite parental magma by an originally F-poor, H<sub>2</sub>O-rich silicate melt within which these elements are relatively insoluble compared to an F-rich melt.

Crystal-liquid fractionation involving feldspars, zircon, apatite, and magnetite could result in a pegmatite melt depleted in Sr, Ba, Fe, HREE, Zr, and Hf. Zircon is a common accessory phase in the potassic series Pikes Peak granite, and Zr is the most depleted of any of the HFSE in the Wellington Lake pegmatite (Fig. 9; Table 6). However, the HFSE- and HREE-enriched South Platte NYF-type pegmatites also formed from the same Pikes Peak granite as the Wellington Lake pegmatite, and the Nd-isotopic compositions of their REE minerals are consistent with the derivation of the pegmatite magma from this granite (Fig. 7; Table 4), but without the HFSE and HREE depletion that would result from crystal-liquid fractionation involving zircon. For the formation of these pegmatites, Simmons and Heinrich (1980) invoked the segregation from the crystallizing granite of a hydrous fluid with a higher concentration of HFSE and HREE than the remaining silicate melt, due to its high F content (London, 2016), thus fractionating additional quantities of these elements into the pegmatite parental magma. We suggest that formation of the Wellington Lake pegmatite also involved an H<sub>2</sub>O-rich silicate melt. This melt included components from a residual melt generated by crystal-liquid fractionation of the crystallizing PPG host. It also contained elements transferred into this melt by an

**Table 6. Estimated bulk composition of the Wellington Lake pegmatite compared to the Pikes Peak Granite and corresponding fractional differences.**

Oxide	WL Model Ox. Wt.%	Granite Ox. Wt.%	Diff. in %
SiO <sub>2</sub>	77.3	75.7	+2.8
TiO <sub>2</sub>	0.0334	0.201	-83.7
Al <sub>2</sub> O <sub>3</sub>	12.2	11.9	+2.1
Fe <sub>2</sub> O <sub>3</sub>	0.859	2.50	-66.4
MnO	0.00515	0.0453	-88.8
MgO	0.0159	0.0235	-33.3
CaO	0.256	0.859	-70.7
Na <sub>2</sub> O	2.75	2.99	-8.8
K <sub>2</sub> O	6.42	5.47	+16.8
P <sub>2</sub> O <sub>5</sub>	0.00432	0.0101	-58.4
Element			
Ga	10.8	10.2	+4.5
Cs	0.94	1.39	-33.2
Ba	75.1	210	-64.8
Rb	406	246	63.5
Sr	8.35	18.1	-54.5
Zr	72.5	532	-86.7
Y	26.7	132	-80.2
Sn	3.36	5.71	-42.2
Nb	23.0	56.4	-60.2
Th	12.9	32.2	-60.9
Hf	3.21	16.2	-80.6
U	4.34	6.41	-34.1
La	70.1	148	-54.1
Ce	133	315	-59.1
Pr	14.3	36.7	-62.3
Nd	46.6	134	-66.3
Sm	7.82	26.1	-70.9
Eu	0.38	0.84	-55.5
Gd	5.05	23.8	-79.4
Tb	0.78	3.92	-80.5
Dy	4.51	24.3	-81.9
Ho	0.92	4.80	-81.3
Er	2.85	13.6	-79.4
Tm	0.49	2.03	-76.5
Yb	3.42	12.7	-73.6
Lu	0.54	1.84	-71.1

H<sub>2</sub>O-rich, but in this case F-poor fluid phase, depleted in elements such as HFSE and REE that are less soluble in an F-poor compared to an F-rich aqueous fluid. This would account for the depletion in the Wellington Lake pegmatite of, for example, Ti and Nb, elements that are not sequestered by the crystallization of zircon or other accessory phases in the PPG.

In contrast to the Wellington Lake pegmatite, the nearby large McGuire pegmatite is enriched in F, Ti, and Nb with abundant fluorite and topaz, and lesser monazite, ilmenite, and niobian rutile (Černý et al., 1999). This peg-

matite exhibits a less-developed concentric zoning and lacks the miarolitic cavities in the core that characterizes the Wellington Lake pegmatite, and its bulk composition is more similar to the large NYF-type pegmatites of the South Platte district. For the McGuire pegmatite, an inward crystallization model of progressively more F- and HFSE-rich melt can explain the late crystallization of the ilmenite and niobian rutile. In the Wellington Lake pegmatite, the observed progressive inward decrease in LREE/HREE of the intermediate zone and so-called “replacement” associations suggest an opposite trend. The trend in the Wellington Lake

pegmatite is of a continuous LREE enrichment during fractional crystallization of an H<sub>2</sub>O-rich and F-poor melt. This results in the final and highly localized crystallization of the LREE minerals fluocerite and bastnäsite from only a small amount of residual F- and CO<sub>2</sub>-rich solution remaining at the top of the pegmatite near the contact of the core and intermediate zones. The late-stage transition of fluocerite to bastnäsite growth in the Wellington Lake pegmatite suggests an increase in pH and/or decrease in F<sup>-</sup>/CO<sub>3</sub><sup>2-</sup> activity ratio (William-Jones and Wood, 1992). The REE zonation seen in the bastnäsite may involve selective complexation of certain REE with CO<sub>3</sub><sup>2-</sup>. The oscillatory zonation observed in the bastnäsite has been seen in late-stage rare-earth element minerals in pegmatites around the world, and may be indicative of locally buffered, rapidly changing chemical environment at the final stages of crystallization (Williams-Jones and Wood, 1992; Gysi et al., 2016).

### Fluid Inclusions

Fluid inclusions at the Wellington Lake pegmatite indicate the presence of at least two compositionally distinct types of fluids: H<sub>2</sub>O-NaCl and H<sub>2</sub>O-CO<sub>2</sub>. H<sub>2</sub>O-NaCl fluid inclusions are only rarely saturated with respect to NaCl, as indicated by the few halite-bearing inclusions. It is possible that the rare higher temperature, high salinity halite-bearing type C, and low salinity vapor-rich type B fluid inclusions represent a distinct earlier fluid of higher temperature boiling fluids as suggested by Simmons and Heinrich (1980), who also observed halite-bearing primary fluid inclusions with homogenization temperatures > 400°C in other South Platte pegmatites. The type-A liquid-rich H<sub>2</sub>O-NaCl fluid inclusions have intermediate salinities and lower temperatures of homogenization.

The inclusions observed in the three quartz samples from Wellington Lake also show some thermometric and compositional similarities and differences with inclusions described by Gagnon et al. (2004) for the Oregon #3 pegmatite in the South Platte region. In both pegmatites, type A two-phase, liquid and vapor, liquid-rich, and also type C three-phase vapor, liquid, and halite inclusions were identified. A third additional type of inclusion rich in CO<sub>2</sub> was also recognized in Wellington Lake, which was not described by Gagnon et al. (2004) for the Oregon #3 pegmatite, but was noted by Simmons and Heinrich (1980) in other South Platte pegmatites. Most significantly, a large proportion of the inclusions from Wellington Lake pegmatite were trapped from solutions of the H<sub>2</sub>O-NaCl ± KCl type as indicated by their eutectic point, which is close to -21°C. In contrast, those from Oregon #3-involved fluids can be characterized as more complex, including both Na + K + Sr + Ba and Na + K + Sr + Ba + Ca solutions as determined by laser ablation-ICP-MS analysis. The Oregon #3

pegmatite also contains fluorite crystals that, according to Gagnon et al. (2004), are associated with REE mineralization, whereas fluorite is not present at Wellington Lake. Fluorite crystals in Oregon #3 also have liquid + vapor inclusions. These contain solutions with Na + K + Sr + Ba as well as REE, Y, Th, and U as measured by LA-ICP-MS analysis, and are, therefore, referred to by Gagnon et al. (2004) as type F4 inclusions.

The two high-temperature types (B and C) of co-existing inclusions are interpreted to be the result of boiling of primary fluids—fluids that precede the ones responsible for lower temperature A-type inclusions (Fig. 8A) as suggested by Simmons and Heinrich (1980) for South Platte district pegmatites. The temperature of all the inclusions in the Wellington Lake pegmatite, with a maximum of 488°C when corrected for pressure, suggests that crystallization took place well below the solidus temperature of an H<sub>2</sub>O-saturated granitic magma. This is consistent with recent models of pegmatite petrogenesis leading to nucleation controlled mega-crystal growth resulting from supercooling (London, 2008). The undercooling and associated nucleation delay also may explain the presence of columbite in the Wellington Lake pegmatite, despite its low total estimated Nb content of ~22 ppm (Table 6). As suggested by London (2016), a pegmatite fluid with < 50 ppm Nb could become saturated and crystallize columbite only below 525°C.

### CONCLUSIONS

We postulate, based on geochemical, mineralogical, and textural evidence, that the Wellington Lake pegmatite formed within the PPG from an H<sub>2</sub>O-rich, but F-poor melt pocket that underwent crystallization associated with supercooling, as suggested to be critical to the development of the characteristic textures and mineralogical zoning of pegmatites (London, 2008, 2014, 2016, 2018). Although the pegmatite melt was derived from the parental PPG magma and had Si, Al, Na, and K contents similar to the PPG magma, it was depleted in other elements such as REE and HFSE, which have low solubility in F-poor silicate melts and aqueous fluids. Processes of zone refinement in the inward-crystallizing pegmatite (London, 2018) could explain the mineralogical zonation observed in the Wellington Lake pegmatite. F and CO<sub>2</sub> played a role only at the last stages of crystallization, when the LREE fluoro and carbonate minerals in the pegmatite core zone crystallized from a low-density silicate melt containing the necessary F, CO<sub>2</sub>, and H<sub>2</sub>O to form these phases as well as create open void spaces in the quartz core.

### ACKNOWLEDGMENTS

We thank Roger Melick for bringing the Wellington Lake pegmatite to our scientific attention, and Jim Hall and

Dean Allum for help in locating the pegmatite. Thanks to Mark Jacobson and Skip Simmons for valuable discussions, and Cal Barnes, Peter Modreski, and Ron Frost for constructive reviews that helped improve the final manuscript. We thank *Rocky Mountain Geology* Managing Editor Brendon Orr and Copy Editor Robert Waggener for editorial assistance. This work was supported in part by the U.S. Geological Survey's Mineral Resources External Research Program grant #G14AP00052.

## REFERENCES CITED

- Allaz, J., Raschke, M.R., Persson, P.M., and Stern, C.R., 2015, Age, petrochemistry, and origin of a REE-rich mineralization in the Longs Peak-St. Vrain batholith, near Jamestown, Colorado (U.S.A.): *American Mineralogist*, v. 100, p. 2,123–2,140.
- Allaz, J.M., Smyth, J.R., Henry, R.E., and four others, 2021, Beryllium-silicon disorder and rare earth crystal chemistry in gadolinite from the White Cloud pegmatite, Colorado, USA: *The Canadian Mineralogist*, v. 58, p. 829–845.
- Allen, O.D., and Comstock, W.J., 1880, Bastnaesite and tysonite from Colorado: *American Journal of Science*, v. 19, p. 390.
- Barker, F., Wones, D.R., Sharp, W.N., and Desborough, O.A., 1975, The Pikes Peak batholith, Colorado Front Range, and a model for the origin of the gabbroanorthosite-syenite-potassic granite suite: *Precambrian Research*, v. 2, p. 97–160.
- Barker, F., Hedge C.E., Millard H.T.J., and O'Neil, J.R., 1976, Pikes Peak batholith: geochemistry of some minor elements and isotopes, and implications for magma genesis, *in* Professional Contributions of Colorado School of Mines: Studies in Colorado Field Geology, v. 8, p. 44–56.
- Berzelius, J., 1818, Basisk flusspatssyradt Cerium, *in* *Ahandlingar i Fysik, Kemi och Mineralogi* [Treatises in Physics, Chemistry and Mineralogy]: Part 6: Stockholm, Sweden, p. 64.
- Beukes, G.J., De Bruijn, H., and Van der Westhuizen, W.A., 1991, Fluocerite and associated minerals from the Bavianskranz granite pegmatite near Kakamas, South Africa: *South African Journal of Geology*, v. 94, p. 313–320.
- Černý, P., and Ercit, T.S., 2005, The classification of granitic pegmatites revisited: *The Canadian Mineralogist*, v. 43, p. 2,005–2,026.
- Černý, P., Chapman, R., Simmons, W.B., and Chackowsky, L.E., 1999, Niobian rutile from the McGuire granitic pegmatite, Park County, Colorado: Solid solution, exsolution, and oxidation: *American Mineralogist*, v. 84, p. 754–763.
- DePaolo, D.J., 1981, Neodymium isotopes in the Colorado Front Range and crust-mantle evolution in the Proterozoic: *Nature*, v. 291, p. 193–196.
- Eby, G.N., 1990, The A-type granitoids: A review of their occurrence and chemical characteristics and speculations on their petrogenesis: *Lithos*, v. 26, p. 115–134.
- Farmer, G.L., Broxton, E.D., Warren, R.G., and Pickthorn, W., 1991, Nd, Sr, and O isotopic variations in metaluminous ash-flow tuffs and related volcanic rocks at Timber Mountain /Oasis Valley Caldera, Complex, SW Nevada: Implication for the origin and evolution of large volume silicic magma bodies: *Contributions to Mineralogy and Petrology*, v. 109, p. 53–68.
- Frost, C.D., and Frost, B.R., 2011, On ferroan (A-type) granitoids: their compositional variability and modes of origin: *Journal of Petrology*, v. 52, p. 39–53.
- Gagnon, J.E., Samson, I.M., Fryer, B.J., and Williams-Jones, A.E., 2004, The composition and origin of hydrothermal fluids in a NYF-type granitic pegmatite, South Platte district, Colorado: Evidence from LA-ICP-MS analysis of fluorite- and quartz-hosted fluid inclusions: *The Canadian Mineralogist*, v. 42, p. 1,331–1,355.
- Geijer, P., 1921, On fluocerite and tysonite: *Geologiska Föreningens i Stockholm Förhandlingar* [Transactions of the Geological Society in Stockholm], v. 43, p. 19–23.
- Glass, J.J., and Smalley, R.G., 1945, Bastnäsite [Gallinas Mountains, New Mexico]: *American Mineralogist*, v. 30, p. 601–615.
- Gordienko, V.V., 1996, Granitnye pegmatity [Granite pegmatites]: St. Petersburg, Russia, St. Petersburg University Press, 271 p. (in Russian).
- Guitreau, M., Mukasa, S.B., Blichert-Toft, J., and Fahnestock, M.F., 2016, Pikes Peak batholith (Colorado, USA) revisited: A SIMS and LA-ICP-MS study of zircon U-Pb ages combined with solution Hf isotopic compositions: *Precambrian Research*, v. 280, p. 179–194.
- Gysi, A., Williams-Jones, A.E., and Collins, P., 2016, Lithochemical vectors for hydrothermal processes in the Strange Lake peralkaline granitic REE-Zr-Nb deposit: *Economic Geology*, v. 111, p. 1,241–1,276.
- Haidinger, W., 1845, *Handbuch der bestimmenden Mineralogie* [Handbook of Determinative Mineralogy]: Vienna, Austria, Braumüller and Seidel, 500 p.
- Haynes, C.V., Jr., 1965, Genesis of the White Cloud and related pegmatites, South Platte area, Jefferson County, Colorado: *Geological Society of America Bulletin*, v. 76, p. 441–462.
- Hidden, W.E., 1891, Remarkable discovery of bastnäsite and tysonite: *American Journal of Science*, third series, v. 41, p. 439.
- Hillebrand, W. F., 1899, Mineralogical notes: Analyses of tysonite, bastnäsite, prosopite, jeffersonite, covellite, etc.: *American Journal of Science*, fourth series, v. 7, p. 51–57.
- Kuzmany, H., 2009, *Solid-state spectroscopy* (second edition): Berlin, Germany, Springer-Verlag, xx + 554 p.
- Lahti, S.I., and Suominen, V., 1988, Occurrence, crystallography and chemistry of the fluocerite-bastnaesite-cerianite intergrowth from the Fjälskär granite, southwestern Finland: *Bulletin of the Geological Society of Finland*, v. 60, p. 45–53.

- London, D., 2008, Pegmatites: The Canadian Mineralogist, Special Publication 10, 347 p.
- \_\_\_\_ 2009, The origin of primary textures in granitic pegmatites: The Canadian Mineralogist, v. 47, p. 697–724.
- \_\_\_\_ 2014, A petrologic assessment of internal zonation in granitic pegmatites: Lithos, v. 184–187, p. 74–104.
- \_\_\_\_ 2015, Reply to Thomas and Davidson on “A petrologic assessment of internal zonation in granitic pegmatites”: Lithos, v. 212–215, p. 469–484.
- \_\_\_\_ 2016, Rare-element granitic pegmatites, *in* Verplanck, P.L., and Hitzman, M.W., Rare earth and critical elements in ore deposits: Littleton, Colorado, Society of Economic Geologists, Reviews in Economic Geology, v. 18, p. 165–194.
- \_\_\_\_ 2018, Ore-forming processes within granitic pegmatites: Ore Geology Reviews, v. 101, p. 349–383.
- Müller, M.M., Kleebe, H.-J., Lauterbach, S., and Zito, G., 2011, Crystallographic orientation relationship between bastnaesite, fluorocerite and cerianite observed in a crystal from the Pikes Peak pegmatites: Z. Kristallogr., v. 226, p. 467–475.
- Potter, R.W., Babcock, R.S., and Brown, D.L., 1977, A new method for determining the solubility of salts in aqueous solutions at elevated temperatures: Journal of Research of the U.S. Geological Survey, v. 5, p. 389–395.
- Potter, R.W., Clyne, M.A., and Brown, D.L., 1978, Freezing point depression of aqueous sodium chloride solutions: Economic Geology, v. 73, p. 284–285.
- Simmons, W.B., Jr., and Heinrich, E.W., 1975, A summary of the petrogenesis of the granite-pegmatite system in the northern end of the Pikes Peak batholith: Fortschritte der Mineralogie [Advances in Mineralogy], v. 52, p. 251–264.
- \_\_\_\_ 1980, Rare earth element pegmatites of the South Platte District, Colorado: Colorado Geological Survey, Resource Series, v. 11, 131 p.
- Simmons, W.B., and Webber, K.L., 2008, Pegmatite genesis: state of the art: European Journal of Mineralogy, v. 20, p. 421–438.
- Simmons, W.B., Lee, M.T., and Brewster, R.H., 1987, Geochemistry and evolution of the South Platte granite-pegmatite system, Jefferson County, Colorado: Geochimica et Cosmochimica Acta [Geochemistry and Cosmochemistry Transactions], v. 51, p. 455–471.
- Simmons, W., Falster, A., Webber, K., and four others, 2016, Bulk composition of Mt. Mica pegmatite, Maine, USA: Implications for the origin of an LCT type pegmatite by anatexis: The Canadian Mineralogist, v. 54, p. 1,043–1,070.
- Sirbescu, M.-L.C., Schmidt, C., Veksler, I.V., and two others, 2017, Experimental crystallization undercooled felsic liquids: Generation of pegmatitic textures: Journal of Petrology, v. 58, p. 539–568.
- Smith, D.R., Noblett, J., Wobus, R.A., and nine others, 1999, Petrology and geochemistry of late-stage intrusions of the A-type, mid-Proterozoic Pikes Peak Batholith (central Colorado, USA): implications for petrogenetic models: Precambrian Research, v. 98, p. 271–305.
- Stilling, A., Cerny, P., and Vanstone, P.J., 2006, The Tanco pegmatite at Bernic Lake, Manitoba. XVI. Zonal and bulk compositions and their petrogenetic significance: The Canadian Mineralogist, v. 44, p. 599–623.
- Swanson, S.E., 1977, Relation of nucleation and crystal-growth rate to the development of granitic textures: American Mineralogist, v. 62, p. 966–978.
- Sverdrup, T.L., Sæbø, P. Chr., and Bryn, K.Ø., 1965, Contributions to the mineralogy of Norway no. 31: Tysonite (fluocerite), a new mineral for Norway: Norsk Geologisk Tidsskrift [Norwegian Journal of Geology], v. 45, p. 177–188.
- Thomas, R., and Davidson, P., 2015, Comment on “A petrologic assessment of internal zonation in granitic pegmatites” by David London (2014): Lithos, v. 212–215, p. 462–468.
- Thomas, R., Davidson, P., and Beurlen, H., 2012, The competing models for the origin and internal evolution of granitic pegmatites in the light of melt and fluid inclusion research: Mineralogy and Petrology, v. 106, p. 55–73.
- Williams-Jones, A.E., and Wood, S.A., 1992, A preliminary petrogenetic grid for REE fluorocarbonates and associated minerals: Geochimica et Cosmochimica Acta [Geochemistry and Cosmochemistry Transactions], v. 56, p. 725–738.
- Zagorsky, V.Y., Makagon, V.M., Shmakin, B.M., and two others, eds., 1997, Granitnye pegmatity (t. 2): Redkometall'nye pegmatity [Granitic pegmatites (v. 2): Rare-metal pegmatites]: Novosibirsk, Russia, Nauka, 420 p. (in Russian).

SCIENTIFIC EDITOR: B. RONALD FROST